

1 **The role of nitrogen and iron biogeochemical cycles on the production and** 2 **export of dissolved organic matter in agricultural headwater catchments**

3 Thibault Lambert¹, Rémi Dupas^{1,*}, Patrick Durand¹

4 ¹ INRAE, UMR SAS 1069, L'Institut Agro, Rennes, France

5 * Corresponding author

6 **Abstract**

7 To better understand the seasonal variations in environmental conditions regulating
8 dissolved organic matter (DOM) export in agricultural headwater catchments, we combined
9 monitoring of nitrate, iron, soluble phosphorus and DOM concentration (as dissolved organic
10 carbon; DOC) and composition (3D fluorescence) in soil and stream waters at regular
11 intervals during one hydrological year. We installed 17 zero-tension lysimeters in organic-rich
12 top soil horizons (15 cm below the surface) in the riparian area of a well-monitored
13 agricultural catchment in French Brittany and collected them at a fortnightly frequency from
14 October 2022 to June 2023. We observed a large increase in DOC concentrations in soil
15 waters during the high flow period linked to the establishment of Fe-reducing conditions and
16 the subsequent release of DOM. We also noted that the timing and the spatial variability in
17 Fe(II) biodissolution in soils was regulated by nitrate from agricultural origin and the
18 heterogeneity of water flow paths at the hillslope scale. Contrary to our current understanding
19 of DOM export in headwater catchments, these results lead us to consider the winter high
20 flow period as an active phase of both DOM production and export.

21 **1. Introduction**

22 Dissolved organic matter (DOM) is a key component of the ecological and biogeochemical
23 functioning of aquatic ecosystems (Hanson et al., 2015), affecting for instance light
24 penetration (Kelly et al., 2001), pollutant transport (Aiken et al., 2011), aquatic microbial
25 metabolism (Wetzel, 1992), and the treatment of drinking waters (Chow et al., 2005). Aquatic
26 DOM, which is mainly of terrestrial origin, represents a fundamental link between the
27 terrestrial, oceanic, and atmospheric compartments of the global carbon cycle (Dean et al.,
28 2020; Battin et al., 2008). Unravelling the sources and drivers of DOM export has become an
29 urgent environmental issue in a context of long-term increasing concentrations of dissolved
30 organic carbon (DOC, a proxy for DOM content) reported in numerous streams in the
31 northern hemisphere (Monteith et al., 2007; De Wit et al., 2021).

32 Numerous research carried out in temperate and boreal regions have shown that headwater
33 catchments are the main entry point of DOM into fluvial networks (Ågren et al., 2007; Creed

34 et al., 2015) and identified riparian areas as the dominant sources of DOM at the catchment
35 scale owing to their location at the terrestrial-aquatic interface (Sanderman et al., 2009;
36 Lambert et al., 2014; Laudon et al., 2012; Winterdahl et al., 2014). Subsurface flow through
37 shallow organic-rich soil layers during storm events (at the daily scale) is responsible for the
38 majority of annual DOC loads (Inamdar et al., 2006), and the DOC *versus* discharge
39 relationships show that DOC export is transport-limited at the event scale (Buffam et al.,
40 2001; Zarnetske et al., 2018). Although geomorphological and climatic conditions regulate
41 DOC loads in aquatic ecosystems (Winterdahl et al., 2014; Laudon et al., 2012), DOM export
42 at the annual scale is commonly conceptualized as a two-steps process in which DOM is
43 produced and stored in the catchment during the hot and dry period, and then exported
44 toward surface waters during the wet and cold period (Boyer et al., 1996). This two-steps
45 conceptual model often described in temperate catchments (Deirmendjian et al., 2018;
46 Strohmeier et al., 2020; Wen et al., 2020; Ruckhaus et al., 2023) is also supported by
47 numerous studies carried out in tropical (Bouillon et al., 2014), boreal (Tiwari et al., 2022),
48 Mediterranean (Butturini and Sabater, 2000) or Arctic fluvial networks (Neff et al., 2006).
49 However the processes regulating the size of the riparian DOM pool remain unclear (Tank et
50 al., 2018 and references below).

51 Antecedent soil conditions of wetness and temperature have been identified as a dominant
52 control on stream DOC with concentrations typically increasing after dry events (Turgeon and
53 Courchesne, 2008; Vázquez et al., 2007; Mehring et al., 2013). Periods of drought promote
54 the production and accumulation of DOM in shallow soil horizons through enhanced soil
55 organic matter decomposition (Harrison et al., 2008; Fenner and Freeman, 2011; Xu and
56 Saiers, 2010), resulting in high stream DOC concentrations during the subsequent rewetting
57 phase of the catchment (Werner et al., 2019; Raymond and Saiers, 2010). In good
58 agreement with this conceptual model is the observation based on long-term data that the
59 mean annual DOC concentrations in streams can be related to the intensity and duration of
60 preceding dry periods (Humbert et al., 2015; Tiwari et al., 2022).

61 However, the establishment of reducing conditions in riparian soils during the winter may
62 have potential implications on our conceptualization of stream DOM export owing to the
63 influence of redox conditions on the iron (Fe) cycle in soils. While particulate Fe-hydroxides
64 absorb organic substances with a high affinity when oxidizing conditions prevail, the
65 microbially-driven dissolution of Fe oxyhydroxides during reducing conditions leads to the
66 release of organic molecules previously bounded to surface minerals (Hagedorn et al., 2000;
67 Blodau et al., 2008). The release of large amounts of DOC in riparian soils during the winter
68 period – considered as non-productive in our current conceptualisation of stream DOM
69 export – has been previously reported (Lambert et al., 2013; Lotfi-Kalahroodi et al., 2021),

70 and several studies have suggested that iron redox cycles may play a major role in
71 catchment-scale DOM export (Knorr, 2013; Selle et al., 2019; Musolff et al., 2017). However,
72 the onset of Fe reducing conditions and the subsequent DOM release could be limited in
73 agricultural catchments owing to large inputs of nitrate (an oxidizing specie) from upslope via
74 groundwater that may prevent Fe reductive biodissolution (Mcmahon and Chapelle, 2008;
75 Christensen et al., 2000).

76 Because most of the studies investigating DOM export in headwater catchments rely on
77 stream water monitoring, the processes regulating the size of the mobile DOM pool in
78 riparian soils and the interaction with other biogeochemical cycles remain largely unknown.
79 We still lack studies investigating how processes occurring in soil waters reflect our
80 conceptualization of solutes dynamics based on observations made in surface waters (Knorr,
81 2013; Dupas et al., 2015; Ledesma et al., 2015; Seibert et al., 2009; Sanderman et al., 2009;
82 Lambert et al., 2013). In this study, we hypothesized that Fe biodissolution may significantly
83 affect DOM release in riparian soils during the winter period with consequences on stream
84 DOM export. We also investigated the potential influence of nitrate from agricultural origin,
85 which may regulate Fe reduction. To this end, we installed zero-tension lysimeters in the
86 riparian area of the Kervidy-Naizin catchment, whose stream waters are continuously
87 monitored for water quality, including DOC at high frequency (Fovet et al., 2018). This
88 catchment is located in Brittany (France), a region where stream DOC concentrations
89 exhibited contrasting trends (increasing, decreasing or no trend) over the 2007-2020 period
90 despite similar geomorphological and climatic conditions (Supplementary Fig. S1). The
91 Kervidy-Naizin catchment for instance exhibits a weak but significant increase in stream
92 DOC concentrations over the last two decades (Strohmenger et al., 2020). In this context,
93 another goal of this study was to explore the hypothesis that long-term regional decrease in
94 nitrate inputs (Abbott et al., 2018) have impacted long-term trends in DOC through iron
95 dynamics in riparian soils. We monitored soil water chemistry during the 2022-2023
96 hydrological year through measurements of DOC, Fe(II) and NO₃ concentrations but also
97 DOM composition (absorbance and fluorescence properties coupled with parallel factor
98 analysis) and soluble reactive phosphorus (SRP) as an additional tracer of Fe reductive
99 dissolution (Gu et al., 2017; Smith et al., 2021). The results allowed us to decipher complex
100 interactions among C, N, and Fe cycles in agricultural catchments and to highlight the
101 occurrence of several processes sustaining DOM export during the winter period.

102 **2. Material and methods**

103 **2.1. Study site**

104 The Kervidy-Naizin research observatory is a 4.9-km² agricultural headwater catchment
105 located in Brittany (western France, Fig. 1). It belongs to the French Critical Zone
106 Observatories (OZCAR) network and is instrumented since the 1970s for the long-term
107 monitoring of the soil-atmosphere-hydrosphere continuum in a context of intensive
108 agriculture (see Fovet et al., 2018 for a complete presentation of the study site).

109 The site is characterized by gentles slopes (<5%) and low elevation that ranges from 98–140
110 m above sea level. The bedrock is composed of impermeable Brioverian schists above which
111 a locally fractured layer of schists is underlain by 1 – 30 m of weathered material and silty
112 loam soils. Soils are well drained except in riparian zones, where water excess leads to
113 hydromorphic, poorly drained soil. Soil organic carbon content presents lateral (riparian
114 *versus* upland soils) and vertical (surface *versus* deep soils) gradients, with highest values
115 about 5.3 – 5.6 % in the uppermost soil horizons (0-20 cm depth) of the riparian area while
116 soil organic content drop under 1% below 20 cm depth (Lambert et al., 2011).

117 The land use is intensive mixed farming, with 91% of the catchment area under agriculture
118 that grows crops to feed a high density of dairy cattle, pigs and poultry. Maize (38%), straw
119 cereals (30%), and grasslands (15%) dominate and wooded areas are mainly confined to
120 valley bottoms along the stream channel or to some hedgerows (Fig. 1).

121 The climate is temperate oceanic, with mean annual temperature of $11.2 \pm 0.6^{\circ}\text{C}$ and mean
122 annual precipitation of 810 ± 180 mm. Precipitation varies seasonally throughout the year,
123 with higher precipitation from October to February (mean monthly precipitation of 92 ± 31
124 mm) and lower precipitation from March to July (mean monthly precipitation of 50 ± 14 mm).
125 The dynamics of the intermittent stream reflects the seasonal pattern of rainfall and
126 evapotranspiration with high discharge periods from November to April and completely dry
127 periods lasting one to three months between July to October depending on the hydrological
128 year.

129 Groundwater level fluctuations are recorded every 15 min along the Kerolland (K) transect,
130 rainfall is monitored at hourly intervals using a weather station located ~ 1400 m from the
131 catchment outlet, and stream discharge is recorded every minute with an automatic gauge
132 station at the outlet of the catchment. A S::SCAN probe is installed at the outlet of the
133 catchment for the measurement of DOC and other variables at high-frequency (Fovet et al.,
134 2018).

135 **2.2. Monitoring and manual sampling**

136 We investigated the seasonal variability in riparian DOM concentration and composition
137 using zero-tension lysimeters designed to collect free soil waters (Supplementary Fig. S2)
138 and installed in September 2022 in topsoil horizons (15 cm depth) in the Kerolland riparian

139 zone, an area known to be a major contributor to stream DOM export in this catchment
140 (Lambert et al., 2014). We placed the lysimeters along three lines parallel to the stream
141 channel, about 10-20 m apart from each other and from the stream, with the aim to capture
142 the heterogeneity of water flow paths and nitrate concentration coming from the upslope
143 cultivated fields. Lysimeters were all located in the hydromorphic soils unit according to the
144 soil map (Fig. 1). We installed 29 zero-tension lysimeters, but some were lost during the
145 study period because of damage by rodents. We kept lysimeters for which at least seven
146 consecutive dates were available, resulting in 17 lysimeters used for the study. We collected
147 soil waters from November 2022 to June 2023 at a weekly to fortnightly frequency depending
148 on the hydro-climatic conditions (Fig. 2). The end of sampling was imposed by the lack of
149 water in lysimeters owing to the gradual drawdown of the water table in the riparian zone
150 during the spring period. We sampled soil waters with a vacuum pump and filtered them at
151 0.2 μm with acetate cellulose syringe encapsulated filters directly on site for all analyses
152 including DOC, NO_3^- , SRP, Fe(II), and DOM composition (absorbance and fluorescence). We
153 used unfiltered water samples to measure physico-chemistry variables including temperature
154 and pH with an ODEON probe. In addition, we collected surface waters right next to the
155 riparian area where lysimeters were located and at the outlet of the catchment. The
156 laboratory analyses were identical for soil and surface waters.

157 **2.3. Analytical procedures**

158 With the exception of Fe(II) measurements that were performed the same day as sampling,
159 all analyses were done within two weeks after sampling. Samples were stored in a 4°C cold
160 room in the dark. Fe(II) analyses were determined using the 1,10-phenanthroline colorimetric
161 method (Lambert et al., 2013): dissolved iron was trapped on site and the optical density of
162 the complex formed with phenanthroline was measured the same day once back to the
163 laboratory at 510 nm with an UV-vis spectrophotometer. DOC concentrations were measured
164 using a total carbon analyzer (SHIMADZU TOC-V) with a precision estimated at $\pm 5\%$ using
165 a standard potassium hydrogen phthalate solution (SIGMA ALDRICH). Nitrate as N-NO_3^- and
166 SRP were determined by spectrometry with an automatic sequential analyzer (SmartChem
167 200, AMS Alliance, France).

168 Absorbance for colored DOM (CDOM) was measured with a Lambda 365 UV/vis
169 spectrophotometer (Perkin Elmer) from 200 to 700 nm (1 nm increment) using a 1 cm quartz
170 cuvette. Samples were diluted in most case due the DOM-rich nature of soil waters. The only
171 purpose of CDOM spectra was to correct excitation-emission matrices (EEMs) for inner filter
172 effects (Ohno, 2002). The dilution factor used for fluorescence measurements were applied
173 to CDOM spectra. Fluorescence DOM (FDOM) was collected as EEMs with a Lambda LS45

174 (Perkin Elmer) using a 1 cm quartz cuvette across excitation wavelengths of 270 – 450 nm (5
175 nm increment) and emission wavelengths of 290 – 600 nm (0.5 nm increment). Samples
176 were diluted so absorbance at 254 nm was below 0.3 to reduce inner filter effects (Ohno,
177 2002).

178 In our study, the Fe(II):DOC ratio was 0.30 ± 0.24 , implying that significant interferences on
179 DOM fluorescence from iron can be expected (Poulin et al., 2014). The degree of iron
180 quenching, however, varies greatly between samples depending on the iron:DOC ratio
181 (Pullin et al., 2007) but also on DOM composition (Jia et al., 2021; Poulin et al., 2014) and
182 Fe(III) concentrations (Ohno et al., 2008), making difficult to predict the influence of Fe on
183 EEMs. That being said, quenching was clearly apparent in some samples ($n < 10$) that
184 showed the fluorescence intensity to increase with dilution factor, reflecting the influence of
185 high level of Fe that reduces DOM fluorescence (Pullin et al., 2007). The quenching
186 impacted EEMs at low (< 270 nm) and moderate to high (420 – 490 nm) excitation and
187 emission wavelengths, respectively, which is consistent with previous studies concluding that
188 Fe mainly impacts fluorescence intensity in EEM locations associated with humic-like
189 fluorophores, namely A and C peaks (Jia et al., 2021; Poulin et al., 2014). Thus, although we
190 cannot rule out an effect of iron on EEMs, this would have impacted the relative contribution
191 of humic-like fluorophores associated with C1 and C2 components of our model (see below)
192 who behaved similarly between clusters and across seasons.

193 **2.4. PARAFAC modelling**

194 EEMs preprocessing (Raman scattering removal and standardization to Raman units) was
195 performed prior to the PARAFAC modeling. Normalization was done using a Milli-Q water
196 sample run the same day as the sample. A five-component PARAFAC model was obtained
197 using the drEEM 0.3.0 Toolbox (Murphy et al., 2013) for MATLAB (MathWorks, Natick, MA,
198 USA). Split-half analysis, random initialization, and visualization of residuals EEMs were
199 used to test and validate the model. The positions of maximum peaks of the PARAFAC
200 components were compared to previous studies carried out in similar context of human-
201 impacted catchments with the open fluorescence database OpenFluor using the OpenFluor
202 add-on for the open-source chromatography software OpenChrom (Murphy et al., 2014). The
203 maximum fluorescence F_{Max} values of each component for a particular sample provided by
204 the model were summed to calculate the total fluorescence signal F_{Tot} of the sample in
205 Raman units. The relative abundance of any particular PARAFAC component X was then
206 calculated as $\%C_X = F_{\text{Max}}(X)/F_{\text{Tot}}$.

207 **2.5 Statistical Analyses**

208 A principal component analysis (PCA) coupled to a clustering analysis was used to
209 discriminate and group lysimeters based on the presence or absence of iron biodissolution in
210 soil waters. The aim was to help visualize temporal pattern for each of the two clusters rather
211 than 17 time series if data were plotted for each lysimeter. For this reason, data (DOC, NO₃,
212 SRP and Fe(II) concentrations and the relative contribution of PARAFAC components) were
213 averaged for each lysimeters then normalized in order to group spatially the lysimeters
214 before investigating temporal patterns. The PCA was performed using the *prcomp* function in
215 the R software, and the *factoextra* package was used to identify the variables that contribute
216 the most to the first two dimensions of the PCA. The cluster analysis, based on the results
217 from the PCA and called Hierarchical Clustering on Principal Components (Josse, 2010),
218 was performed with the *FactoMineR* package for R (Lê et al., 2008). Relationships between
219 variables were investigated either through Pearson or Spearman correlations depending of
220 the nature (linear or not) of the correlations.

221 3. Results

222 3.1. Hydro-climatic context

223 The hydrological regime of the study site is characterized by a succession of three distinct
224 periods determined by water table fluctuations along the hillslope, corresponding to different
225 hydrological regimes for the riparian soils (Fig. 2; Lambert et al., 2013): (i) a period of
226 progressive rewetting of riparian soils after the dry season and of low groundwater flow and
227 low stream discharge (01/09/2022 – 18/12/2022, mean and cumulated precipitation = 5.1 ± 5.3
228 mm d⁻¹ and 338.5 mm, respectively); (ii) a period of prolonged waterlogging of riparian soils
229 induced by the rise of the water table in the upland domain, corresponding to high values of
230 hillslope groundwater flow and stream discharge (18/12/2022 – 9/05/2023, mean and
231 cumulated precipitation = 6.8 ± 7.9 mm d⁻¹ and 573 mm, respectively); and (iii) a period of
232 drainage and progressive drying of the riparian soils induced by the drawdown first in the
233 upland domain then in the bottomland domain and corresponding to the decrease of both the
234 hillslope groundwater flow and stream discharge (09/05/2023 – 01/07/2023, mean and
235 cumulated precipitation = 4.3 ± 4.4 mm d⁻¹ and 42.5 mm, respectively). Air temperature (Fig.
236 2C) showed a smoothed seasonal variability with decreasing values from September to
237 December (from ~20°C to -2°C) followed by a rise in temperature from 0°C to 20°C from
238 February to July. This pattern was only interrupted by a relatively short episode of higher
239 temperature (close to 10°C) during the winter, coinciding with the first intense rainfall period
240 of the year.

241 3.2. Fluorescence properties of DOM

242 Five PARAFAC components were identified in soil waters (Supplementary Fig. S3), all of
243 which already described in previous studies. All five components had humic-like fluorescence
244 properties (Fellman et al., 2010). Components C1 (excitation/emission peaks = 350 nm /444
245 nm), C2 (<270/450), and C5 (410/488) predominantly cover the regions of EEMs associated
246 with peaks A and C and are common tracers of terrestrially-derived DOM in surface waters
247 (Kothawala et al., 2015; Stedmon and Markager, 2005; Logozzo et al., 2023; Lambert et al.,
248 2017) while C3 (330/406) and C4 (295/410) are both located near the classical peak M,
249 indicating a microbial transformation of terrestrial DOM (Williams et al., 2010; Lambert et al.,
250 2022; Yamashita et al., 2010). The maximum fluorescence intensity of all components were
251 strongly related to DOC concentrations (not shown) and the relative contribution of each
252 component decreased from as C1 (29.7 ± 3.1 %) > C2 (28.3 ± 3.6 %) > C3 (19.5 ± 2.5 %) > C4
253 (12.9 ± 6.6 %) > C5 (9.7 ± 2.1 %).

254 **3.3. Seasonal variations in soil and stream waters**

255 Temperature in soil waters (Fig. 3A) followed the same pattern as air temperature: values
256 oscillated between 5°C and 15°C during November – January, reached minimums between 4
257 and 7 °C in January – March and then increased gradually during the end of the study period
258 up to 18 – 20 °C in June. pH varied between 6.2 and 7.4 (mean 6.9 ± 0.3) across lysimeters
259 and didn't exhibit significant trends over the study period (Fig. 3B). Solutes, however,
260 exhibited complex patterns with a high variability across lysimeters and time, especially
261 during the high flow period (Fig. 3C-F). Despite the fact that lysimeters were installed along
262 three lines ranging 10-30 m from the stream, no spatial pattern was identified. Overall, these
263 elements were strongly linked to each other (Fig. 4). DOC concentrations ranged from 2.3 to
264 87.4 mg L^{-1} (mean = $30.2 \pm 12.8 \text{ mg L}^{-1}$) over the study period and were linearly and positively
265 (Pearson $r = 0.73$, p value < 0.0001) associated with Fe(II) that ranged from 0 to 45.8 mg L^{-1}
266 (mean = $9.8 \pm 7.6 \text{ mg L}^{-1}$). Fe(II) was negatively (Spearman $r = -0.56$, p value < 0.0001)
267 correlated with NO_3 (from 0 to 16.4 mg L^{-1} , mean = $0.9 \pm 1.1 \text{ mg L}^{-1}$), and SRP (from 0 to 0.5
268 mg L^{-1} , mean = $0.1 \pm 0.1 \text{ mg L}^{-1}$) was also positively (Pearson $r = 0.21$, p value = 0.0005)
269 related to Fe(II), but not as strongly as for DOC.

270 DOC concentrations in stream waters varied from 2.9 to 36.8 mg L^{-1} during the study period
271 (Fig. 5). Maximum concentrations were reached during storm events due to a rapid response
272 to rainfall and the mobilisation of riparian wetland waters (Durand and Juan Torres, 1996).
273 There was a tendency for minimum (at base flow) and maximum (at peak discharge)
274 concentrations to decrease from November to March. From March to July, however, minimal
275 concentrations remained stable while maximum values showed a slight increasing trend.

276 **3.4. Clustering of soil waters**

277 The first two components of the PCA explained 69.4 % of the total variance of the data and
278 discriminated lysimeters depending on the presence or absence of Fe(II) biodissolution in
279 soil waters of the riparian area (Fig. 6). The first principal component (PC1, 54% of the total
280 variance) was mainly related to NO₃ concentrations and terrestrial humic-like components
281 (C1, C2, and C5) on positive scores, and to DOC and Fe(II) concentrations and the microbial
282 humic-like component C4 on negative scores. The second component (PC2, 15.4% of the
283 total variance) was related to SRP (positive score) and the component C3 (negative score).
284 PARAFAC components had similar or even higher scores than DOC, Fe(II), and NO₃
285 concentrations on the two first dimensions of the PCA (Supplementary Fig. S4), illustrating
286 the importance of DOM composition as an important factor contributing to explain the spatial
287 variability across lysimeters. The distribution of PARAFAC components along the first
288 dimension reflects the relationships between their relative contribution and Fe(II),
289 concentrations (not shown). More specifically, %C4 was strongly and positively correlated
290 with Fe(II) ($R^2 = 0.38$, Pearson $r = 0.62$) compared to other components that exhibited
291 weakest and negative relationships with Fe(II) (R^2 from 0.09 to 0.19, Pearson r from -0.30 to
292 -0.43). In other words, lysimeters capturing Fe biodissolution in the riparian area were
293 associated with high DOC and a greater proportion of the microbial C4 component compared
294 to lysimeters enriched in nitrate where no Fe(II) was measured.

295 The hierarchical clustering based on the PCA results grouped the lysimeters in two distinct
296 clusters based on the presence (cluster 1) or absence (cluster 2) of Fe(II) (Fig. 6). This
297 approach allowed us to gain insight into the temporal evolution of solutes in soil waters since
298 clear patterns appeared once the data were grouped by cluster (Fig. 7). In cluster 1, DOC, N-
299 NO₃ and SRP decreased from 39.8 ± 13.3 to 23.4 ± 8.4 mg L⁻¹, from 2.6 ± 3.6 to 1.2 ± 1.8 mg L⁻¹,
300 and from 0.18 ± 0.18 to 0.08 ± 0.15 mg L⁻¹, respectively, during the rewetting phase of the
301 catchment while Fe(II) was not measured at significant levels. During the high flow period,
302 however, Fe(II) increased gradually from 3.7 ± 3.2 to 26.5 ± 7.8 mg L⁻¹, and both DOC and SRP
303 followed a similar trend with concentrations raising from 27.3 ± 9.5 to 54.9 ± 25.0 mg L⁻¹ and
304 from 0.07 ± 0.13 to 0.18 ± 0.11 mg L⁻¹, respectively. During this period and until the end of the
305 hydrological cycle, N-NO₃ were very low, decreasing from 0.54 ± 0.66 mg L⁻¹ at the beginning
306 of the high flow period to values below 0.15 mg L⁻¹ the rest of the survey. The start of the
307 third hydrological period corresponding to the drawdown of the water table and the
308 consecutive aeration of riparian soils was marked by the rapid drop of Fe(II) at 8.1 ± 7.4 mg L⁻¹,
309 DOC at 17.5 ± 10.9 mg L⁻¹, and SRP at 0.02 ± 0.02 mg L⁻¹.

310 Similarly to cluster 1, soil waters from the cluster 2 exhibited a decline in DOC and SRP
311 concentrations during the rewetting phase of the catchment but these trends continued
312 during the high flow period, with minimal values reached in the middle of February. Thus,

313 DOC dropped from 34.5 ± 7.1 to 9.4 ± 3.1 mg L⁻¹ and SRP from 0.19 ± 0.08 to 0.02 ± 0.01 mg L⁻¹
314 during this period, before showing an increasing trend to reach concentrations about
315 21.0 ± 6.1 mg L⁻¹ for DOC and 0.16 ± 0.13 mg L⁻¹ for SRP at the end of the high flow period.
316 DOC remained elevated (24.1 ± 3.1 mg L⁻¹) at the start of the dry period, but SRP dropped
317 close to depletion. In contrast, N-NO₃ first increased from 0.57 ± 0.81 mg L⁻¹ in November to
318 maximum values of 6.5 ± 5.9 mg L⁻¹ in the middle of March, and then exhibited decreasing
319 concentrations until a complete depletion at the beginning of the third hydrological period.
320 Contrary to cluster 1, Fe(II) was not measured at significant concentrations in cluster 2 (*i.e.*
321 below 0.5 mg L⁻¹) except in March, during which Fe(II) increased from 1.2 ± 1.9 to 4.1 ± 0.2 mg
322 L⁻¹.

323 4. Discussion

324 4.1. The buffering effect of nitrate on iron reductive dissolution

325 The reductive biodissolution of iron during the high-water winter period is a recurrent process
326 in riparian soils of headwater catchments (Smolders et al., 2017; Knorr, 2013; Selle et al.,
327 2019). The magnitude of variations in Fe(II) and associated DOC and SRP dynamics
328 reported in this study are in line with previous works conducted in the same research
329 catchment (Lambert et al., 2013; Lotfi-Kalahroodi et al., 2021; Gu et al., 2017). In addition,
330 our results evidenced a marked variability in the intensity of iron dissolution across lysimeters
331 that we attributed to the spatial distribution of NO₃-rich water flow paths that can inhibit and
332 delay the release of Fe(II) and DOC in soil waters.

333 A fundamental condition for the establishment of reductive conditions is the prolonged
334 waterlogging of riparian soils. As shown earlier for this and other lowland catchments on
335 impervious bedrock, the increase of the hydraulic gradient induced by the rise of
336 groundwater in the upland domain during the high flow period maintains a strong hydrologic
337 connection between upland and riparian domains (Pacific et al., 2010; Molenat et al., 2008).
338 Under these conditions, riparian soils remain waterlogged owing to a high and continuous
339 hillslope groundwater flow, leading to the gradual establishment of reductive conditions and
340 the subsequent triggering of Fe-biodissolution as long as inputs of oxidizing species
341 remained limited and/or counterbalanced by higher rate of consumption through microbial
342 activity (Lotfi-Kalahroodi et al., 2021; Lambert et al., 2013). This pattern is well illustrated by
343 data from lysimeters of the first cluster (Fig. 7). After a quick depletion of an initial stock of
344 nitrate accumulated during the previous summer, reductive conditions were rapidly
345 established at the beginning of the high flow period and increasing Fe(II) concentrations in
346 soil waters lead to the onset of the reductive Fe biodissolution in riparian soils. The gradual
347 increase in Fe(II) during all the high flow period despite variations in temperature or rainfall

348 patterns (with some intense precipitation events $> 20 \text{ mm d}^{-1}$) suggests a limited impact of
349 these climatic episodes, except during a period of low precipitation during which both Fe(II)
350 and DOC exhibited a slight decrease in February/March. We attributed this small drop to the
351 drawdown of the water table in upland groundwater flow following a prolonged absence of
352 precipitations (see PK3 fluctuations, Fig. 2) that may have re-oxygenated soil waters (as no
353 changes in N-NO₃ occurred).

354 Therefore, large release of DOC occurred in soils of the first cluster. Iron biodissolution also
355 affected SRP, but the relationships was weaker suggesting that the reductive dissolution of
356 soil Fe was not the primary driver of SRP concentrations in soils. For instance, soil
357 properties, and more specifically soil phosphorus content and speciation, have been shown
358 to strongly regulate SRP in soil waters of the Kervidy-Naizin catchment (Gu et al., 2017).
359 Regarding DOC, the mean DOC:Fe(II) molar ratio was 142.4 ± 285.5 . This was higher than
360 the DOC:Fe(II) ratio measured in experimental conditions (74.5 ± 74.6) but similar to value
361 measured on the field (134.4 ± 25.6) by Lotfi-Kalahroodi et al. (2021) who aimed to investigate
362 Fe reduction in the riparian area of our study catchment. Fe(III) concentrations in soil waters
363 were not measured, but, based on the work of Lotfi-Kalahroodi et al. (2021), we can estimate
364 a ratio between total Fe and Fe(II) of 4.8. Keeping in mind that this is a rough estimation, our
365 mean DOC:Fe ratio would be about 29.3 ± 58.8 , which is consistent with previous studies (e.g.
366 Selle et al., 2019; Musolff et al., 2017; Grybos et al., 2009; Cabezas et al., 2013). The nature
367 of processes releasing DOC upon the reduction of soil-Fe oxyhydroxides in riparian soils of
368 our study site has been studied in laboratory conditions (Grybos et al., 2009). Results have
369 shown that up to 60% of the release is due to DOC desorption caused by the pH increase
370 that accompanies the reduction of Feoxyhydroxides in these soils, the remaining 40% being
371 due to the dissolution of Fe-oxyhydroxides that strongly adsorb organic compounds
372 previously bounded to surface minerals (e.g. Hagedorn et al., 2000). In good agreement with
373 these results, soil DOC was positively related to pH (Supplementary Fig. S5). The abrupt
374 decrease in DOC in June illustrates the restoration of aerobic conditions owing to the
375 drawdown of the water table in the bottomland domain led to the formation of Fe-minerals
376 and the subsequent retention of DOC and SRP (Gu et al., 2017).

377 Lysimeters from the second cluster showed a very different pattern. Although some of them
378 were located close (3-4 m) to lysimeters in which reducing conditions prevailed, there was no
379 evidence of Fe(II) release, arguably because of the presence of nitrate. Indeed, and in
380 agreement with studies carried out in wetland (Lucassen et al., 2004) and lacustrine
381 (Andersen, 1982) sediments, we argue that the Fe-biodissolution biodissolution was inhibited
382 as long as long as NO₃ remained in sufficient quantity in soil waters. In the absence of such
383 production or regeneration process, both DOC and SRP showed a net depletion pattern from

384 November to March. The influence of nitrate as a buffer of Fe-biodissolution was furthermore
385 supported by the observation of a slight release of Fe(II) in May, at a moment when nitrate
386 became depleted from soil waters, probably because of plant uptake. Interestingly, we found
387 that the threshold value of nitrate above which the process is activated (based on the NO₃
388 *versus* Fe(II) relationship (Fig. 4) as well as timing of Fe-biodissolution identified in cluster 1
389 and cluster 2) ranged between 1.2 and 1.8 N-NO₃ (4.1 – 6.2 mg L⁻¹), which is close to the
390 threshold value of 6 mg L⁻¹ established at the catchment scale by Musolff et al. (2017) in
391 German streams.

392 The PARAFAC components identified in the model suggest a dominance of highly aromatic
393 and conjugated molecules across all lysimeters and dates, which is typical of DOM derived
394 from soil organic matter and found in poorly drained soils in riparian or wetland areas
395 (Sanderman et al., 2009; Lambert et al., 2013; Yamashita et al., 2010). The larger proportion
396 of C4 in the first cluster however indicates that the Fe oxyhydroxides reduction leads to
397 greater proportion of microbially-derived compounds within the DOM pool. In agreement with
398 previous studies showing that the Fe(III) reduction could enhance the decomposition of
399 organic matter in soils (Chen et al., 2020; Kappler et al., 2021), the close link between Fe(II)
400 and C4 likely reflects an indirect effect of Fe biodissolution promoting the degradation of soil
401 OM and the subsequent incorporation of microbially-derived compounds into the DOM pool
402 (Dong et al., 2023). This hypothesis is well consistent with previous experimental studies
403 performed with soils from the Kervidy-Naizin riparian area, which showed that bacterial
404 reduction of Fe(III)-oxides to Fe(II) was concomitant with the release of large biological
405 organic by-products upon the growth of bacterial communities (Lotfi-Kalahroodi et al., 2021).

406 Our study evidences a strong spatial heterogeneity of the establishment of reducing
407 conditions in the riparian area of the Kervidy-Naizin catchment, associated with differences in
408 the composition of DOM released in soil waters. It remain to be determined, however, the
409 reason for such variability in biogeochemical processes in riparian soils. A first explanation
410 can be related to the heterogeneity in water flowpaths in soils. In intensive agricultural
411 catchments such as our study site, inflow of NO₃-rich water may arise from the rise of
412 contaminated groundwater in valley bottom s and/or from subsurface flow paths that connect
413 upland soils to riparian soils (Molenat et al., 2008). It is likely that lysimeters from the second
414 cluster captured preferential flow paths of NO₃-rich waters while lysimeters from the first
415 cluster were disconnected from those preferential water circulations. Alternatively, the
416 absence of nitrate in soil waters may arise from a higher rate of denitrification that
417 counterbalanced NO₃ inputs. Research based on field observation remained limited to
418 decipher the respective role of hydrology *versus* biogeochemistry in controlling Fe(II)

419 biodissolution in riparian soils, and experimental studies would be required to provide more
420 quantitative values on these potential drivers and their interactions.

421 **4.2. Implication for stream DOM export at the catchment scale**

422 The current understanding of DOM export in headwater catchments is based on a two-steps
423 conceptual model, in which a pool of mobile DOM is built in soils during the dry season and
424 then flushed towards surface waters during the following wet season (e.g. Tiwari et al., 2022;
425 Ruckhaus et al., 2023; Strohmenger et al., 2020; Raymond and Saiers, 2010). However, the
426 high-frequency measurements of DOC in the stream do not fully support this statement. The
427 establishment of a hydrological connection between riparian soils and the stream during the
428 winter period showed the stream DOC to gradually decrease both at peak discharge during
429 successive storm events and at base flow during inter-storm periods (Figure 5). This pattern,
430 which repeats every year in this catchment (Strohmenger et al., 2020), is well consistent with
431 the hypothesis of the mobilisation and exhaustion of a DOM pool limited in size built during
432 the summer period (Humbert et al., 2015). However, stream DOC were found to increase
433 slightly in March/April after the low-flow period that showed the hydrological connection
434 between soils and the stream to decrease. It is unlikely that the mobilisation of an additional
435 pool of DOM from upland soils may explain this small raises in stream DOC because this
436 pool is 1) relatively small in terms of size, and 2) quickly exhausted at the beginning of the
437 winter period (Lambert et al., 2014). Therefore, the seasonal pattern of stream DOC likely
438 reflects the regeneration of the riparian DOM pool during the winter period as shown by our
439 data collected in soil waters of riparian wetlands.

440 Stable carbon isotopes have indeed demonstrated that riparian soils of the Kervidy-Naizin
441 catchment – and more particularly the DOM-rich uppermost soil horizons – are the dominant
442 source of stream DOC at the catchment scale (Lambert et al., 2014), a feature commonly
443 shared by headwater catchments (e.g. Sanderman et al., 2009). Thus, the decline in DOC
444 and SRP observed in soil waters, particularly in the second cluster whereby these elements
445 became almost depleted (Fig. 7), was consistent with the general flushing behaviour of the
446 catchment shown by stream DOC from November to February. Similarly, the large two to
447 three fold increase in DOC concentrations in riparian soils (in cluster 1 and 2, respectively)
448 denotes a large mobilisation of DOM between March and May despite wet and low
449 temperature conditions, that could explain in turn the pattern observed in stream DOC at the
450 same time. While part of this regeneration can be attributed to iron biodissolution, the release
451 of large amount of DOC the cluster 2 where the reductive biodissolution of Fe(III) was limited
452 implies that another production mechanisms contributed to release DOM in riparian soils. It is
453 unlikely that agricultural inputs (crop residues, manure application, etc) main may explain the

454 increases in the riparian area, as these sources are episodic and/or size-limited (Lambert et
455 al., 2014; Humbert et al., 2015; Pacific et al., 2010). This observation echoes previous works
456 on the Kervidy-Naizin catchment showing effective inter-annual regeneration mechanisms of
457 the pool of soluble phosphorus in soils unrelated to iron dynamics (Gu et al., 2017), a
458 statement supported here by the fact that SRP concentrations followed a similar pattern as
459 DOC in soils grouped in the second cluster (Fig. 7).

460 The PARAFAC results suggest that DOM mobilized from soil to streams is only composed by
461 aromatic molecules of high molecular weight. Although complex organic molecules indeed
462 dominate stream DOM export (Fellman et al., 2009), it should be noted however that protein-
463 like components are commonly found in stream waters (Inamdar et al., 2012), including in
464 our study site (Humbert et al., 2020). The lack of such components in our model results from
465 our sampling approach and not from their absence in catchment soils. Indeed, the production
466 of protein-like components in catchment soils is restricted to the summer hot and dry period
467 during which a pool made of low-aromatic and microbially-derived compounds built up in
468 riparian soils (Lambert et al., 2013). However, this DOM pool is quickly flushed and
469 exhausted during the rewetting phase in October-November, and soil DOM during the winter
470 period is mainly composed by highly-aromatic molecules originating from soil organic
471 material (Lambert et al., 2014). Agricultural practices such as fertilizer applications can
472 represent another source of protein-like DOM in the catchment (Humbert et al., 2020), but
473 these inputs remain episodic with a low impact on DOM at the catchment scale (Humbert et
474 al., 2015; Lambert et al., 2014). For instance, a recent one-year of monitoring of soil waters
475 at different locations in the catchment has shown that protein-like components represent only
476 $3.44 \pm 2.8\%$ of the total fluorescence signal in catchment soils, this contribution being
477 particularly low in riparian areas (Humbert et al., 2020). Therefore, the absence of protein-
478 like components in our PARAFAC model is the consequence of our sampling design that
479 focused on DOM production mechanisms in riparian soils (distant from agricultural inputs)
480 during the winter period (period of production of highly aromatic compounds in soils).

481 Taking together, our results have two important implications regarding our conceptualisation
482 of DOM export in headwater catchments. First, it challenges the idea that the wet period acts
483 solely as a passive export period for DOM, with no or little DOM production (Strohmenger et
484 al., 2020; Ruckhaus et al., 2023; Wen et al., 2020). Second, it emphasizes that stream DOC
485 dynamics at the outlet is an integrative signal, potentially masking the high spatial
486 heterogeneity of the system owing to complex interactions between biogeochemical cycles in
487 soils, nutrient transfer at the soil/stream interface and hydrological functioning of catchments.
488 While the patterns of stream DOC were consistent with that observed in soils, our study
489 remains however limited in its capacity to quantify the relative contribution of the cluster

490 identified to stream DOC export. Additionally, we do not have the necessary data such as
491 isotopes or molecular markers to elucidate the precise origin and DOM (and SRP) release in
492 soils unrelated to iron biodissolution, and this should be the focus of future work combining
493 experimental and field studies.

494 **Conclusion**

495 The combined monitoring of soil and stream waters in a temperate headwater catchment
496 allowed us to evidence the dual role of high flow period as both an active phase of DOM
497 production and export. In agreement with previous studies (e.g. Selle et al., 2019; Knorr,
498 2013), the establishment of Fe-reducing conditions in riparian areas was identified as a major
499 mechanism for the release of large amount of DOM in soil waters. In agricultural catchments,
500 however, we found that this process can be buffered by nitrate, leading to a strong spatial
501 heterogeneity in the magnitude of iron biodissolution and its consequences on soil DOM
502 dynamics. Our study also evidenced that another production mechanisms unrelated to Fe
503 dynamics contributed to release DOM in riparian soils during the winter period, pointing to
504 the need to further investigate stream DOC export at the soil/stream interface.

505 The interactions between the N and Fe biogeochemical cycles may have potential
506 implications regarding long-term increases in DOC in streams of Brittany. Indeed, stream
507 DOC in the Kervidy-Naizin catchment has been slowly but significantly increasing in the last
508 two decades, and this trend is mirrored by a decline in NO₃ concentrations (Strohmenger et
509 al., 2020). While part of the DOC trend can be related to changes in climatic conditions as
510 winters tend to wetter over the years (Strohmenger et al., 2020), the long-term decline in N
511 inputs from agriculture may have favoured the increase in stream DOC by enhancing Fe(II)
512 biodissolution in riparian soils. This hypothesis could partly explain why catchments having
513 similar geomorphological and climatic properties present contrasting long-term trends at the
514 scale of the Brittany region (Supplementary Fig. S1). Indeed, nitrate concentrations have
515 largely decreased during the last decades, but the rate of recovery is not uniform across the
516 region (Abbott et al., 2018). Studies carried out at the regional scale aiming to decipher the
517 interactions between local (agricultural practices) and global (climatic conditions) and the
518 consequences on stream DOC export would be critical considering the influence of DOM on
519 water quality and on the ecological and biogeochemical functioning of surface waters.

520 **Data availability**

521 Data on soil waters will be published on Zenodo.org upon the reservation that the paper will
522 be accepted for publication. Hydrological and climatic data from the Kervidy-Naizin site are
523 available here: https://geosass.fr/web/?page_id=103.

524 **Acknowledgements**

525 We thank Militza G., Harald F., P. Petitjean and Celine B. for their assistance in field and lab
526 work. We thank the Associate Editor J.-H. Park, and W. Clayton, B. Selle and one anonymous
527 reviewer for constructive comments on the previous version of the manuscript.

528 **Financial support**

529 This study has received funding from the H2020 European Research Council under the Marie
530 Skłodowska-Curie grant agreement COSTREAM No 101064945.

531 **Author contribution**

532 TL conceived the study. TL defined protocols with contribution from RD and PD. TL collected
533 field samples with help from RD. TL made laboratory analysis. TL analysed the data and
534 drafted the manuscript with inputs from RD and PD. All authors contributed and approved to
535 the manuscript.

536 **Competing interests**

537 The authors declare that they have no conflict of interest.

538 **References**

- 539 Abbott, B. W., Moatar, F., Gauthier, O., Fovet, O., Antoine, V., and Ragueneau, O.: Trends and
540 seasonality of river nutrients in agricultural catchments: 18years of weekly citizen science in France,
541 Science of The Total Environment, 624, 845-858, <https://doi.org/10.1016/j.scitotenv.2017.12.176>,
542 2018.
- 543 Ågren, A., Buffam, I., Jansson, M., and Laudon, H.: Importance of seasonality and small streams for the
544 landscape regulation of dissolved organic carbon export, Journal of Geophysical Research:
545 Biogeosciences, 112, <https://doi.org/10.1029/2006JG000381>, 2007.
- 546 Aiken, G. R., Hsu-Kim, H., and Ryan, J. N.: Influence of Dissolved Organic Matter on the Environmental
547 Fate of Metals, Nanoparticles, and Colloids, Environmental Science & Technology, 45, 3196-3201,
548 10.1021/es103992s, 2011.
- 549 Andersen, J. M.: Effect of nitrate concentration in lake water on phosphate release from the sediment,
550 Water Research, 16, 1119-1126, [https://doi.org/10.1016/0043-1354\(82\)90128-2](https://doi.org/10.1016/0043-1354(82)90128-2), 1982.
- 551 Battin, T. J., Kaplan, L. A., Findlay, S., Hopkinson, C. S., Marti, E., Packman, A. I., Newbold, J. D., and
552 Sabater, F.: Biophysical controls on organic carbon fluxes in fluvial networks, Nature Geoscience,
553 1, 95-100, 10.1038/ngeo101, 2008.
- 554 Blodau, C., Fulda, B., Bauer, M., and Knorr, K.-H.: Arsenic speciation and turnover in intact organic soil
555 mesocosms during experimental drought and rewetting, Geochimica et Cosmochimica Acta, 72,
556 3991-4007, <https://doi.org/10.1016/j.gca.2008.04.040>, 2008.
- 557 Bouillon, S., Yambele, A., Gillikin, D. P., Teodoru, C., Darchambeau, F., Lambert, T., and Borges, A. V.:
558 Contrasting biogeochemical characteristics of the Oubangui River and tributaries (Congo River
559 basin), Sci Rep, 4, 5402, 10.1038/srep05402, 2014.
- 560 Boyer, E. W., Hornberger, G. M., Bencala, K. E., and McKnight, D.: Overview of a simple model
561 describing variation of dissolved organic carbon in an upland catchment, Ecological Modelling, 86,
562 183-188, [https://doi.org/10.1016/0304-3800\(95\)00049-6](https://doi.org/10.1016/0304-3800(95)00049-6), 1996.
- 563 Buffam, I., Galloway, J. N., Blum, L. K., and McGlathery, K. J.: A stormflow/baseflow comparison of
564 dissolved organic matter concentrations and bioavailability in an Appalachian stream,
565 Biogeochemistry, 53, 269-306, 10.1023/A:1010643432253, 2001.
- 566 Butturini, A. and Sabater, F.: Seasonal variability of dissolved organic carbon in a Mediterranean stream,
567 Biogeochemistry, 51, 303-321, 10.1023/A:1006420229411, 2000.

568 Chen, C., Hall, S. J., Coward, E., and Thompson, A.: Iron-mediated organic matter decomposition in
569 humid soils can counteract protection, *Nature Communications*, 11, 2255, 10.1038/s41467-020-
570 16071-5, 2020.

571 Chow, A. T., Gao, S., and Dahlgren, R. A.: Physical and chemical fractionation of dissolved organic
572 matter and trihalomethane precursors: A review, *Journal of Water Supply: Research and
573 Technology-Aqua*, 54, 475-507, 10.2166/aqua.2005.0044, 2005.

574 Christensen, T. H., Bjerg, P. L., Banwart, S. A., Jakobsen, R., Heron, G., and Albrechtsen, H.-J.:
575 Characterization of redox conditions in groundwater contaminant plumes, *Journal of Contaminant
576 Hydrology*, 45, 165-241, [https://doi.org/10.1016/S0169-7722\(00\)00109-1](https://doi.org/10.1016/S0169-7722(00)00109-1), 2000.

577 Creed, I. F., McKnight, D. M., Pellerin, B. A., Green, M. B., Bergamaschi, B. A., Aiken, G. R., Burns, D.
578 A., Findlay, S. E. G., Shanley, J. B., Striegl, R. G., Aulenbach, B. T., Clow, D. W., Laudon, H.,
579 McGlynn, B. L., McGuire, K. J., Smith, R. A., and Stackpole, S. M.: The river as a chemostat: fresh
580 perspectives on dissolved organic matter flowing down the river continuum, *Canadian Journal of
581 Fisheries and Aquatic Sciences*, 72, 1272-1285, 10.1139/cjfas-2014-0400, 2015.

582 de Wit, H. A., Stoddard, J. L., Monteith, D. T., Sample, J. E., Austnes, K., Couture, S., Fölster, J.,
583 Higgins, S. N., Houle, D., Hruška, J., Krám, P., Kopáček, J., Paterson, A. M., Valinia, S., Van Dam,
584 H., Vuorenmaa, J., and Evans, C. D.: Cleaner air reveals growing influence of climate on dissolved
585 organic carbon trends in northern headwaters, *Environmental Research Letters*, 16, 104009,
586 10.1088/1748-9326/ac2526, 2021.

587 Dean, J. F., Meisel, O. H., Martyn Rosco, M., Marchesini, L. B., Garnett, M. H., Lenderink, H., van
588 Logtestijn, R., Borges, A. V., Bouillon, S., Lambert, T., Röckmann, T., Maximov, T., Petrov, R.,
589 Karsanaev, S., Aerts, R., van Huissteden, J., Vonk, J. E., and Dolman, A. J.: East Siberian Arctic
590 inland waters emit mostly contemporary carbon, *Nature Communications*, 11, 1627,
591 10.1038/s41467-020-15511-6, 2020.

592 Deirmendjian, L., Loustau, D., Augusto, L., Lafont, S., Chipeaux, C., Poirier, D., and Abril, G.: Hydro-
593 ecological controls on dissolved carbon dynamics in groundwater and export to streams in a
594 temperate pine forest, *Biogeosciences*, 15, 669-691, 10.5194/bg-15-669-2018, 2018.

595 Dong, H., Zeng, Q., Sheng, Y., Chen, C., Yu, G., and Kappler, A.: Coupled iron cycling and organic
596 matter transformation across redox interfaces, *Nature Reviews Earth & Environment*, 4, 659-673,
597 10.1038/s43017-023-00470-5, 2023.

598 Dupas, R., Gruau, G., Gu, S., Humbert, G., Jaffrézic, A., and Gascuel-Oudou, C.: Groundwater control
599 of biogeochemical processes causing phosphorus release from riparian wetlands, *Water Research*,
600 84, 307-314, <https://doi.org/10.1016/j.watres.2015.07.048>, 2015.

601 Durand, P. and Juan Torres, J. L.: Solute transfer in agricultural catchments: the interest and limits of
602 mixing models, *Journal of Hydrology*, 181, 1-22, [https://doi.org/10.1016/0022-1694\(95\)02922-2](https://doi.org/10.1016/0022-1694(95)02922-2),
603 1996.

604 Fellman, J. B., Hood, E., and Spencer, R. G. M.: Fluorescence spectroscopy opens new windows into
605 dissolved organic matter dynamics in freshwater ecosystems: A review, *Limnology and
606 Oceanography*, 55, 2452-2462, <https://doi.org/10.4319/lo.2010.55.6.2452>, 2010.

607 Fellman, J. B., Hood, E., D'Amore, D. V., Edwards, R. T., and White, D.: Seasonal changes in the
608 chemical quality and biodegradability of dissolved organic matter exported from soils to streams in
609 coastal temperate rainforest watersheds, *Biogeochemistry*, 95, 277-293, 10.1007/s10533-009-
610 9336-6, 2009.

611 Fenner, N. and Freeman, C.: Drought-induced carbon loss in peatlands, *Nature Geoscience*, 4, 895-
612 900, 10.1038/ngeo1323, 2011.

613 Fovet, O., Ruiz, L., Gruau, G., Akkal, N., Aquilina, L., Busnot, S., Dupas, R., Durand, P., Faucheux, M.,
614 Fauvel, Y., Fléchar, C., Gilliet, N., Grimaldi, C., Hamon, Y., Jaffrezic, A., Jeanneau, L., Labasque,
615 T., Le Henaff, G., Mérot, P., Molénat, J., Petitjean, P., Pierson-Wickmann, A.-C., Squidant, H.,
616 Viaud, V., Walter, C., and Gascuel-Oudou, C.: AgrHyS: An Observatory of Response Times in
617 Agro-Hydro Systems, *Vadose Zone Journal*, 17, 180066, <https://doi.org/10.2136/vzj2018.04.0066>,
618 2018.

619 Grybos, M., Davranche, M., Gruau, G., Petitjean, P., and Pédrot, M.: Increasing pH drives organic matter
620 solubilization from wetland soils under reducing conditions, *Geoderma*, 154, 13-19,
621 <https://doi.org/10.1016/j.geoderma.2009.09.001>, 2009.

622 Gu, S., Gruau, G., Dupas, R., Rumpel, C., Crème, A., Fovet, O., Gascuel-Oudou, C., Jeanneau, L.,
623 Humbert, G., and Petitjean, P.: Release of dissolved phosphorus from riparian wetlands: Evidence
624 for complex interactions among hydroclimate variability, topography and soil properties, *Science of
625 The Total Environment*, 598, 421-431, <https://doi.org/10.1016/j.scitotenv.2017.04.028>, 2017.

626 Hagedorn, F., Kaiser, K., Feyen, H., and Schleppe, P.: Effects of Redox Conditions and Flow Processes
627 on the Mobility of Dissolved Organic Carbon and Nitrogen in a Forest Soil, *Journal of Environmental*
628 *Quality*, 29, 288-297, <https://doi.org/10.2134/ieq2000.00472425002900010036x>, 2000.

629 Hanson, P. C., Pace, M. L., Carpenter, S. R., Cole, J. J., and Stanley, E. H.: Integrating Landscape
630 Carbon Cycling: Research Needs for Resolving Organic Carbon Budgets of Lakes, *Ecosystems*,
631 18, 363-375, 10.1007/s10021-014-9826-9, 2015.

632 Harrison, A. F., Taylor, K., Scott, A., Poskitt, J., Benham, D., Grace, J., Chaplow, J., and Rowland, P.:
633 Potential effects of climate change on DOC release from three different soil types on the Northern
634 Pennines UK: examination using field manipulation experiments, *Global Change Biology*, 14, 687-
635 702, <https://doi.org/10.1111/j.1365-2486.2007.01504.x>, 2008.

636 Humbert, G., Jaffrezic, A., Fovet, O., Gruau, G., and Durand, P.: Dry-season length and runoff control
637 annual variability in stream DOC dynamics in a small, shallow groundwater-dominated agricultural
638 watershed, *Water Resources Research*, 51, 7860-7877, <https://doi.org/10.1002/2015WR017336>,
639 2015.

640 Humbert, G., Parr, T. B., Jeanneau, L., Dupas, R., Petitjean, P., Akkal-Corfini, N., Viaud, V., Pierson-
641 Wickmann, A.-C., Denis, M., Inamdar, S., Gruau, G., Durand, P., and Jaffrézic, A.: Agricultural
642 Practices and Hydrologic Conditions Shape the Temporal Pattern of Soil and Stream Water
643 Dissolved Organic Matter, *Ecosystems*, 23, 1325-1343, 10.1007/s10021-019-00471-w, 2020.

644 Inamdar, S., Finger, N., Singh, S., Mitchell, M., Levia, D., Bais, H., Scott, D., and McHale, P.: Dissolved
645 organic matter (DOM) concentration and quality in a forested mid-Atlantic watershed, USA,
646 *Biogeochemistry*, 108, 55-76, 10.1007/s10533-011-9572-4, 2012.

647 Inamdar, S. P., O'Leary, N., Mitchell, M. J., and Riley, J. T.: The impact of storm events on solute exports
648 from a glaciated forested watershed in western New York, USA, *Hydrological Processes*, 20, 3423-
649 3439, <https://doi.org/10.1002/hyp.6141>, 2006.

650 Jia, K., Manning, C. C. M., Jollymore, A., and Beckie, R. D.: Technical note: Effects of iron(II) on
651 fluorescence properties of dissolved organic matter at circumneutral pH, *Hydrol. Earth Syst. Sci.*,
652 25, 4983-4993, 10.5194/hess-25-4983-2021, 2021.

653 Josse, J.: Principal component methods - hierarchical clustering - partitional clustering: why would we
654 need to choose for visualizing data?,

655 Kappler, A., Bryce, C., Mansor, M., Lueder, U., Byrne, J. M., and Swanner, E. D.: An evolving view on
656 biogeochemical cycling of iron, *Nature Reviews Microbiology*, 19, 360-374, 10.1038/s41579-020-
657 00502-7, 2021.

658 Kelly, D. J., Clare, J. J., and Bothwell, M. L.: Attenuation of solar ultraviolet radiation by dissolved organic
659 matter alters benthic colonization patterns in streams, *Journal of the North American Benthological*
660 *Society*, 20, 96-108, 10.2307/1468191, 2001.

661 Knorr, K. H.: DOC-dynamics in a small headwater catchment as driven by redox fluctuations and
662 hydrological flow paths – are DOC exports mediated by iron reduction/oxidation cycles?,
663 *Biogeosciences*, 10, 891-904, 10.5194/bg-10-891-2013, 2013.

664 Kothawala, D. N., Ji, X., Laudon, H., Ågren, A. M., Futter, M. N., Köhler, S. J., and Tranvik, L. J.: The
665 relative influence of land cover, hydrology, and in-stream processing on the composition of
666 dissolved organic matter in boreal streams, *Journal of Geophysical Research: Biogeosciences*,
667 120, 1491-1505, <https://doi.org/10.1002/2015JG002946>, 2015.

668 Lambert, T., Perolo, P., Escoffier, N., and Perga, M. E.: Enhanced bioavailability of dissolved organic
669 matter (DOM) in human-disturbed streams in Alpine fluvial networks, *Biogeosciences*, 19, 187-200,
670 10.5194/bg-19-187-2022, 2022.

671 Lambert, T., Pierson-Wickmann, A.-C., Gruau, G., Thibault, J.-N., and Jaffrezic, A.: Carbon isotopes as
672 tracers of dissolved organic carbon sources and water pathways in headwater catchments, *Journal*
673 *of Hydrology*, 402, 228-238, <https://doi.org/10.1016/j.jhydrol.2011.03.014>, 2011.

674 Lambert, T., Bouillon, S., Darchambeau, F., Morana, C., Roland, F. A. E., Descy, J.-P., and Borges, A.
675 V.: Effects of human land use on the terrestrial and aquatic sources of fluvial organic matter in a
676 temperate river basin (The Meuse River, Belgium), *Biogeochemistry*, 136, 191-211,
677 10.1007/s10533-017-0387-9, 2017.

678 Lambert, T., Pierson-Wickmann, A.-C., Gruau, G., Jaffrezic, A., Petitjean, P., Thibault, J.-N., and
679 Jeanneau, L.: Hydrologically driven seasonal changes in the sources and production mechanisms
680 of dissolved organic carbon in a small lowland catchment, *Water Resources Research*, 49, 5792-
681 5803, <https://doi.org/10.1002/wrcr.20466>, 2013.

682 Lambert, T., Pierson-Wickmann, A. C., Gruau, G., Jaffrezic, A., Petitjean, P., Thibault, J. N., and
683 Jeanneau, L.: DOC sources and DOC transport pathways in a small headwater catchment as
684 revealed by carbon isotope fluctuation during storm events, *Biogeosciences*, 11, 3043-3056,
685 10.5194/bg-11-3043-2014, 2014.

686 Laudon, H., Buttle, J., Carey, S. K., McDonnell, J., McGuire, K., Seibert, J., Shanley, J., Soulsby, C.,
687 and Tetzlaff, D.: Cross-regional prediction of long-term trajectory of stream water DOC response
688 to climate change, *Geophysical Research Letters*, 39, <https://doi.org/10.1029/2012GL053033>,
689 2012.

690 Lê, S., Josse, J., and Husson, F.: FactoMineR: An R Package for Multivariate Analysis, *Journal of*
691 *Statistical Software*, 25, 1 - 18, 10.18637/jss.v025.i01, 2008.

692 Ledesma, J. L. J., Grabs, T., Bishop, K. H., Schiff, S. L., and Köhler, S. J.: Potential for long-term transfer
693 of dissolved organic carbon from riparian zones to streams in boreal catchments, *Global Change*
694 *Biology*, 21, 2963-2979, <https://doi.org/10.1111/gcb.12872>, 2015.

695 Logozzo, L. A., Hosen, J. D., McArthur, J., and Raymond, P. A.: Distinct drivers of two size fractions of
696 operationally dissolved iron in a temperate river, *Limnology and Oceanography*, 68, 1185-1200,
697 <https://doi.org/10.1002/lno.12338>, 2023.

698 Lotfi-Kalahroodi, E., Pierson-Wickmann, A.-C., Rouxel, O., Marsac, R., Bouhnik-Le Coz, M., Hanna, K.,
699 and Davranche, M.: More than redox, biological organic ligands control iron isotope fractionation in
700 the riparian wetland, *Scientific Reports*, 11, 1933, 10.1038/s41598-021-81494-z, 2021.

701 Lucassen, E. C. H. E. T., Smolders, A. J. P., van der Salm, A. L., and Roelofs, J. G. M.: High groundwater
702 nitrate concentrations inhibit eutrophication of sulphate-rich freshwater wetlands, *Biogeochemistry*,
703 67, 249-267, 10.1023/B:BIOG.0000015342.40992.cb, 2004.

704 McMahon, P. B. and Chapelle, F. H.: Redox Processes and Water Quality of Selected Principal Aquifer
705 Systems, *Groundwater*, 46, 259-271, <https://doi.org/10.1111/j.1745-6584.2007.00385.x>, 2008.

706 Mehring, A. S., Lowrance, R. R., Helton, A. M., Pringle, C. M., Thompson, A., Bosch, D. D., and Vellidis,
707 G.: Interannual drought length governs dissolved organic carbon dynamics in blackwater rivers of
708 the western upper Suwannee River basin, *Journal of Geophysical Research: Biogeosciences*, 118,
709 1636-1645, <https://doi.org/10.1002/2013JG002415>, 2013.

710 Molenat, J., Gascuel-Oudou, C., Ruiz, L., and Gruau, G.: Role of water table dynamics on stream nitrate
711 export and concentration in agricultural headwater catchment (France), *Journal of Hydrology*, 348,
712 363-378, <https://doi.org/10.1016/j.jhydrol.2007.10.005>, 2008.

713 Monteith, D. T., Stoddard, J. L., Evans, C. D., de Wit, H. A., Forsius, M., Høgåsen, T., Wilander, A.,
714 Skjelkvåle, B. L., Jeffries, D. S., Vuorenmaa, J., Keller, B., Kopáček, J., and Vesely, J.: Dissolved
715 organic carbon trends resulting from changes in atmospheric deposition chemistry, *Nature*, 450,
716 537-540, 10.1038/nature06316, 2007.

717 Murphy, K. R., Stedmon, C. A., Graeber, D., and Bro, R.: Fluorescence spectroscopy and multi-way
718 techniques. PARAFAC, *Analytical Methods*, 5, 6557-6566, 10.1039/C3AY41160E, 2013.

719 Murphy, K. R., Stedmon, C. A., Wenig, P., and Bro, R.: OpenFluor— an online spectral library of auto-
720 fluorescence by organic compounds in the environment, *Analytical Methods*, 6, 658-661,
721 10.1039/C3AY41935E, 2014.

722 Musolff, A., Selle, B., Büttner, O., Opitz, M., and Tittel, J.: Unexpected release of phosphate and organic
723 carbon to streams linked to declining nitrogen depositions, *Global Change Biology*, 23, 1891-1901,
724 <https://doi.org/10.1111/gcb.13498>, 2017.

725 Neff, J. C., Finlay, J. C., Zimov, S. A., Davydov, S. P., Carrasco, J. J., Schuur, E. A. G., and Davydova,
726 A. I.: Seasonal changes in the age and structure of dissolved organic carbon in Siberian rivers and
727 streams, *Geophysical Research Letters*, 33, <https://doi.org/10.1029/2006GL028222>, 2006.

728 Ohno, T.: Fluorescence Inner-Filtering Correction for Determining the Humification Index of Dissolved
729 Organic Matter, *Environmental Science & Technology*, 36, 742-746, 10.1021/es0155276, 2002.

730 Ohno, T., Amirbahman, A., and Bro, R.: Parallel Factor Analysis of Excitation–Emission Matrix
731 Fluorescence Spectra of Water Soluble Soil Organic Matter as Basis for the Determination of
732 Conditional Metal Binding Parameters, *Environmental Science & Technology*, 42, 186-192,
733 10.1021/es071855f, 2008.

734 Pacific, V. J., Jencso, K. G., and McGlynn, B. L.: Variable flushing mechanisms and landscape structure
735 control stream DOC export during snowmelt in a set of nested catchments, *Biogeochemistry*, 99,
736 193-211, 10.1007/s10533-009-9401-1, 2010.

737 Poulin, B. A., Ryan, J. N., and Aiken, G. R.: Effects of Iron on Optical Properties of Dissolved Organic
738 Matter, *Environmental Science & Technology*, 48, 10098-10106, 10.1021/es502670r, 2014.

739 Pullin, M. J., Anthony, C., and Maurice, P. A.: Effects of Iron on the Molecular Weight Distribution, Light
740 Absorption, and Fluorescence Properties of Natural Organic Matter, *Environmental Engineering*
741 *Science*, 24, 987-997, 10.1089/ees.2006.0040, 2007.

742 Raymond, P. A. and Saiers, J. E.: Event controlled DOC export from forested watersheds,
743 *Biogeochemistry*, 100, 197-209, 10.1007/s10533-010-9416-7, 2010.

744 Ruckhaus, M., Seybold, E. C., Underwood, K. L., Stewart, B., Kincaid, D. W., Shanley, J. B., Li, L., and
745 Perdrial, J. N.: Disentangling the responses of dissolved organic carbon and nitrogen

746 concentrations to overlapping drivers in a northeastern United States forested watershed, *Frontiers*
747 *in Water*, 5, 10.3389/frwa.2023.1065300, 2023.

748 Sanderman, J., Lohse, K. A., Baldock, J. A., and Amundson, R.: Linking soils and streams: Sources and
749 chemistry of dissolved organic matter in a small coastal watershed, *Water Resources Research*,
750 45, <https://doi.org/10.1029/2008WR006977>, 2009.

751 Seibert, J., Grabs, T., Köhler, S., Laudon, H., Winterdahl, M., and Bishop, K.: Linking soil- and stream-
752 water chemistry based on a Riparian Flow-Concentration Integration Model, *Hydrol. Earth Syst.*
753 *Sci.*, 13, 2287-2297, 10.5194/hess-13-2287-2009, 2009.

754 Selle, B., Knorr, K.-H., and Lischeid, G.: Mobilisation and transport of dissolved organic carbon and iron
755 in peat catchments—Insights from the Lehstenbach stream in Germany using generalised additive
756 models, *Hydrological Processes*, 33, 3213-3225, <https://doi.org/10.1002/hyp.13552>, 2019.

757 Smith, G. J., McDowell, R. W., Condon, L. M., Daly, K., Ó hUallacháin, D., and Fenton, O.: Reductive
758 dissolution of phosphorus associated with iron-oxides during saturation in agricultural soil profiles,
759 *Journal of Environmental Quality*, 50, 1207-1219, <https://doi.org/10.1002/jeq2.20256>, 2021.

760 Smolders, E., Baetens, E., Verbeeck, M., Nawara, S., Diels, J., Verdievel, M., Peeters, B., De Cooman,
761 W., and Baken, S.: Internal Loading and Redox Cycling of Sediment Iron Explain Reactive
762 Phosphorus Concentrations in Lowland Rivers, *Environmental Science & Technology*, 51, 2584-
763 2592, 10.1021/acs.est.6b04337, 2017.

764 Stedmon, C. A. and Markager, S.: Resolving the variability in dissolved organic matter fluorescence in
765 a temperate estuary and its catchment using PARAFAC analysis, *Limnology and Oceanography*,
766 50, 686-697, <https://doi.org/10.4319/lo.2005.50.2.0686>, 2005.

767 Strohmenger, L., Fovet, O., Akkal-Corfini, N., Dupas, R., Durand, P., Faucheux, M., Gruau, G., Hamon,
768 Y., Jaffrezic, A., Minaudo, C., Petitjean, P., and Gascuel-Oudou, C.: Multitemporal Relationships
769 Between the Hydroclimate and Exports of Carbon, Nitrogen, and Phosphorus in a Small Agricultural
770 Watershed, *Water Resources Research*, 56, e2019WR026323,
771 <https://doi.org/10.1029/2019WR026323>, 2020.

772 Tank, S. E., Fellman, J. B., Hood, E., and Kritzberg, E. S.: Beyond respiration: Controls on lateral carbon
773 fluxes across the terrestrial-aquatic interface, *Limnology and Oceanography Letters*, 3, 76-88,
774 <https://doi.org/10.1002/lol2.10065>, 2018.

775 Tiwari, T., Sponseller, R. A., and Laudon, H.: The emerging role of drought as a regulator of dissolved
776 organic carbon in boreal landscapes, *Nature Communications*, 13, 5125, 10.1038/s41467-022-
777 32839-3, 2022.

778 Turgeon, J. M. L. and Courchesne, F.: Hydrochemical behaviour of dissolved nitrogen and carbon in a
779 headwater stream of the Canadian Shield: relevance of antecedent soil moisture conditions,
780 *Hydrological Processes*, 22, 327-339, <https://doi.org/10.1002/hyp.6613>, 2008.

781 Vázquez, E., Romani, A. M., Sabater, F., and Butturini, A.: Effects of the Dry–Wet Hydrological Shift on
782 Dissolved Organic Carbon Dynamics and Fate Across Stream–Riparian Interface in a
783 Mediterranean Catchment, *Ecosystems*, 10, 239-251, 10.1007/s10021-007-9016-0, 2007.

784 Wen, H., Perdrial, J., Abbott, B. W., Bernal, S., Dupas, R., Godsey, S. E., Harpold, A., Rizzo, D.,
785 Underwood, K., Adler, T., Sterle, G., and Li, L.: Temperature controls production but hydrology
786 regulates export of dissolved organic carbon at the catchment scale, *Hydrol. Earth Syst. Sci.*, 24,
787 945-966, 10.5194/hess-24-945-2020, 2020.

788 Werner, B. J., Musolff, A., Lechtenfeld, O. J., de Rooij, G. H., Oosterwoud, M. R., and Fleckenstein, J.
789 H.: High-frequency measurements explain quantity and quality of dissolved organic carbon
790 mobilization in a headwater catchment, *Biogeosciences*, 16, 4497-4516, 10.5194/bg-16-4497-
791 2019, 2019.

792 Wetzel, R. G.: Gradient-dominated ecosystems: sources and regulatory functions of dissolved organic
793 matter in freshwater ecosystems, *Hydrobiologia*, 229, 181-198, 10.1007/BF00007000, 1992.

794 Williams, C. J., Yamashita, Y., Wilson, H. F., Jaffé, R., and Xenopoulos, M. A.: Unraveling the role of
795 land use and microbial activity in shaping dissolved organic matter characteristics in stream
796 ecosystems, *Limnology and Oceanography*, 55, 1159-1171,
797 <https://doi.org/10.4319/lo.2010.55.3.1159>, 2010.

798 Winterdahl, M., Erlandsson, M., Futter, M. N., Weyhenmeyer, G. A., and Bishop, K.: Intra-annual
799 variability of organic carbon concentrations in running waters: Drivers along a climatic gradient,
800 *Global Biogeochemical Cycles*, 28, 451-464, <https://doi.org/10.1002/2013GB004770>, 2014.

801 Xu, N. and Saiers, J. E.: Temperature and Hydrologic Controls on Dissolved Organic Matter Mobilization
802 and Transport within a Forest Topsoil, *Environmental Science & Technology*, 44, 5423-5429,
803 10.1021/es1002296, 2010.

804 Yamashita, Y., Scinto, L. J., Maie, N., and Jaffé, R.: Dissolved Organic Matter Characteristics Across a
805 Subtropical Wetland's Landscape: Application of Optical Properties in the Assessment of
806 Environmental Dynamics, *Ecosystems*, 13, 1006-1019, 10.1007/s10021-010-9370-1, 2010.
807 Zarnetske, J. P., Bouda, M., Abbott, B. W., Saiers, J., and Raymond, P. A.: Generality of Hydrologic
808 Transport Limitation of Watershed Organic Carbon Flux Across Ecoregions of the United States,
809 *Geophysical Research Letters*, 45, 11,702-711,711, <https://doi.org/10.1029/2018GL080005>, 2018.

810

811 **Figure Caption**

812 **Figure 1** – Location map of the Kervidy-Naizin experimental catchment showing land uses.
813 Hatched areas located along the stream channel network indicate the extent of hydromorphic
814 soils commonly waterlogged during the winter period. Lysimeters were located downslope the
815 piezometer PK1.

816 **Figure 2** – (A) Record of hourly discharge and daily rainfall, (B) record of hourly piezometric
817 levels in wetland (PK1) and upland (PK3) domains, and (C) record of daily air temperature.
818 Black triangles in panel A indicate fieldwork for manual sampling of soil and stream waters.
819 Vertical black dashed lines delimit the different hydrologic periods, namely the rewetting, high
820 flow, and recession phases. See text for details.

821 **Figure 3** – Evolution of (A) air temperature and (B) pH, (C) DOC, (D) NO₃, (E) Fe(II), and (F)
822 SRP in soil waters during the study period. Vertical black dashed lines delimit the different
823 hydrologic periods, namely the rewetting, high flow, and recession phases. See text for details.

824 **Figure 4** – Relationships between (A) DOC and Fe(II), (B) Fe(II) and NO₃, and (C) SRP and
825 Fe(II) in soil waters during the study period.

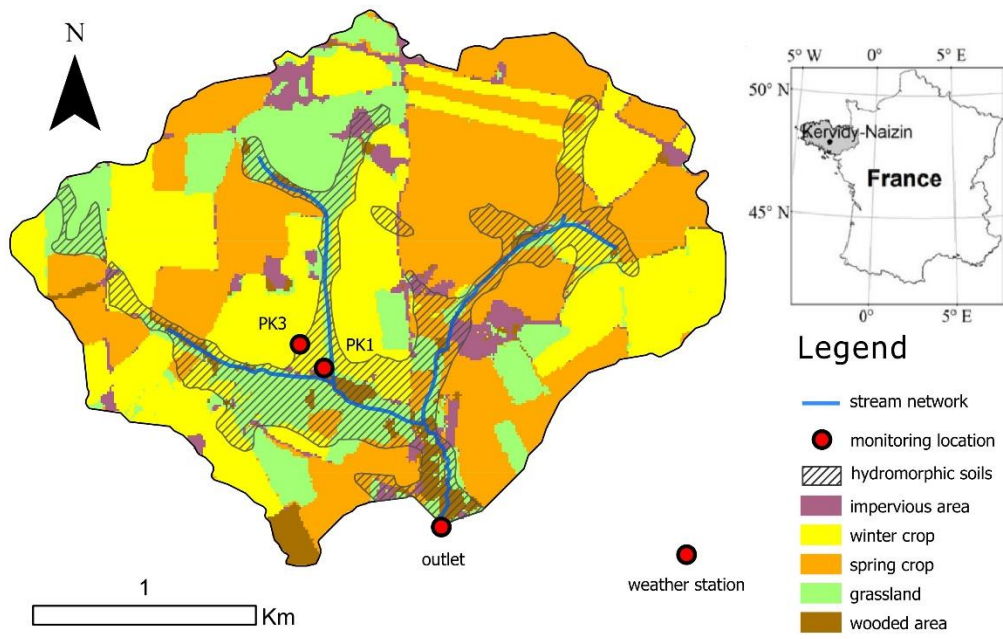
826 **Figure 5** – Variations in stream DOC measured at high frequency at the outlet of the
827 catchment. Vertical black dashed lines delimit the different hydrologic periods, namely the
828 rewetting, high flow, and recession phases. See text for details.

829 **Figure 6** – PCA biplot, including loadings plot for the input variables and scores plot for
830 lysimeters. One point represents one lysimeters, PCA being based on average values
831 calculated over the study period. Markers are coloured according to the cluster identified by
832 the Hierarchical Clustering on Principal Components (see material and methods).

833 **Figure 7** – Evolution of (A) DOC, (B) Fe(II), (C) NO₃, and (D) SRP in soil waters for each
834 cluster. Lysimeters are grouped according the Hierarchical Clustering on Principal
835 Components (see text for details and Fig. 6). Vertical black dashed lines delimit the different
836 hydrologic periods, namely the rewetting, high flow, and recession phases. See text for details.

837

839 **Figure 1**



840

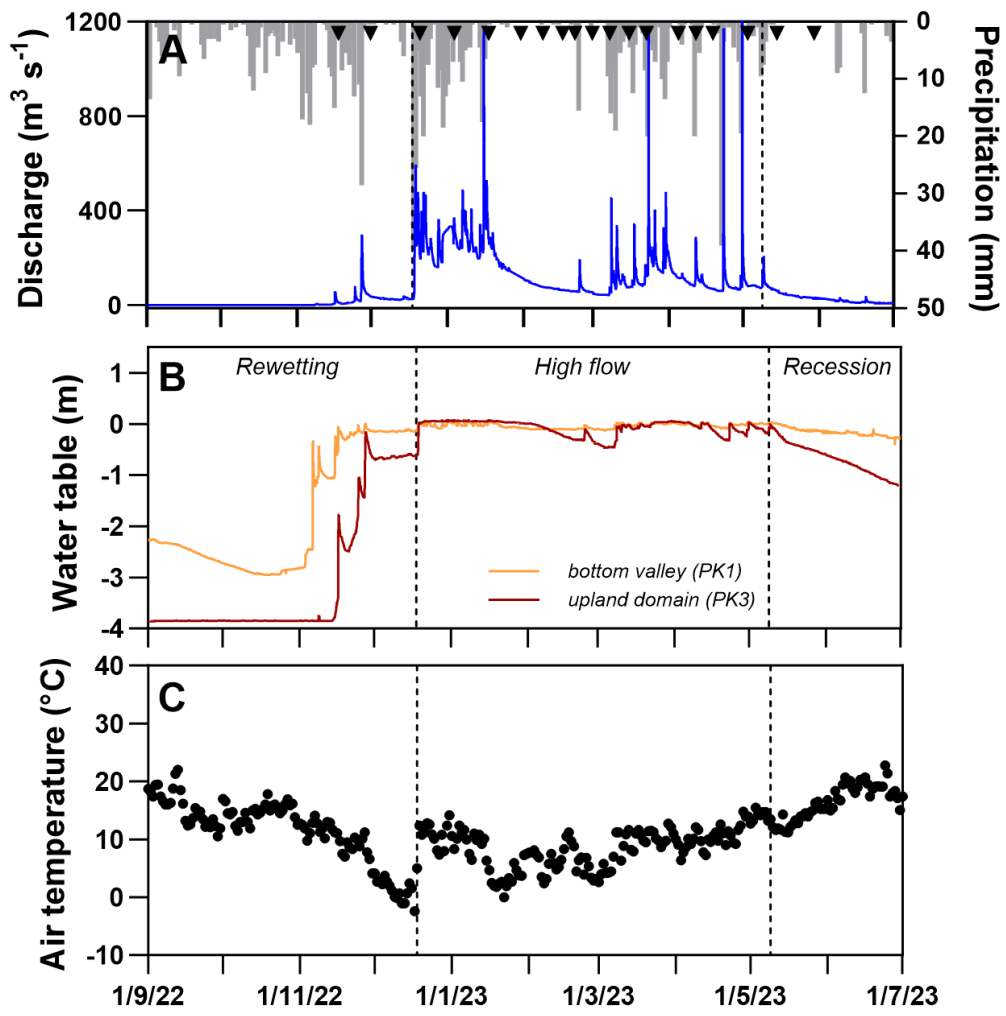
841

842

843

844

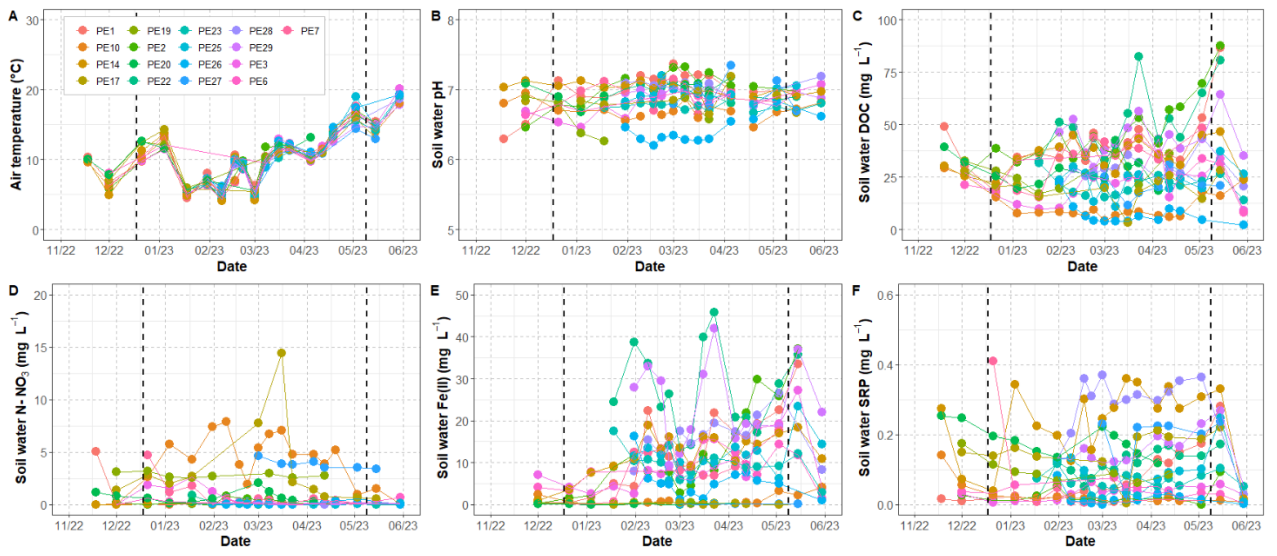
845 **Figure 2**



846

847

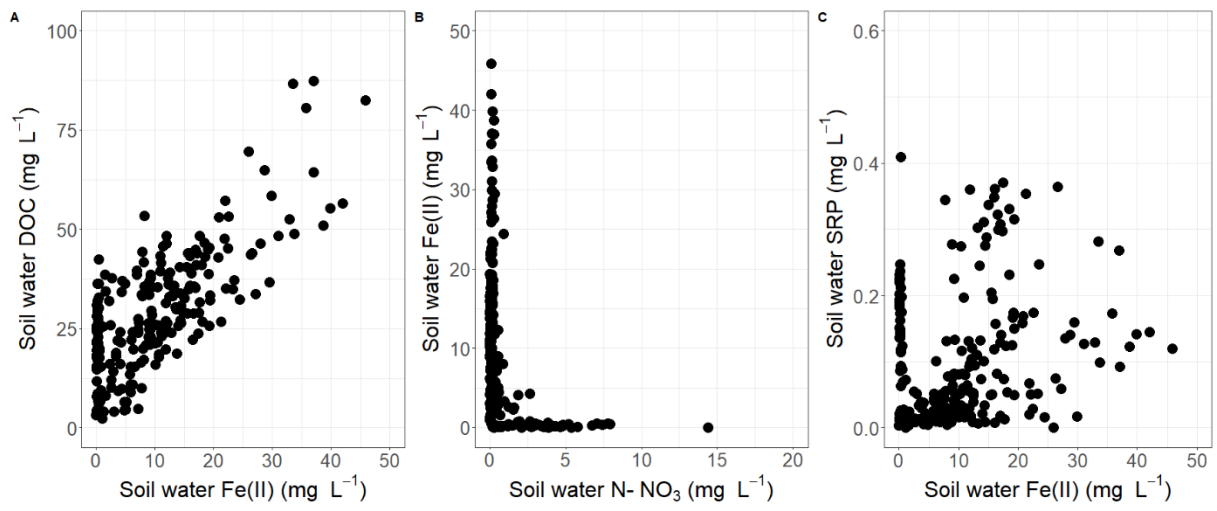
848 **Figure 3**



849

850

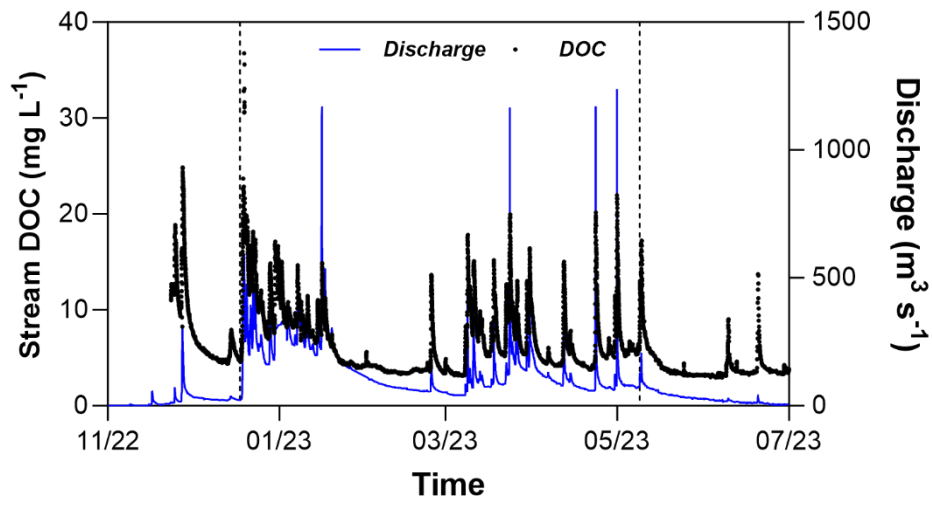
851 **Figure 4**



852

853

854 **Figure 5**

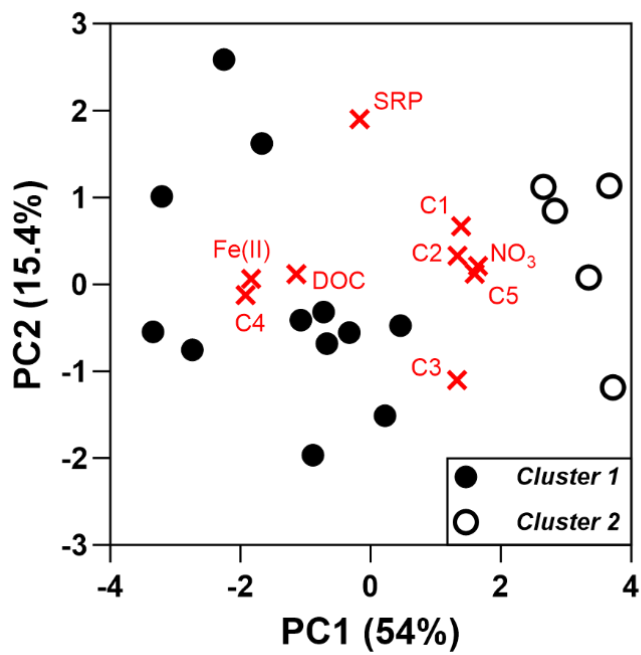


855

856

857

858 **Figure 6**



859

860

861

